*31st EPS Conference on Plasma Phys. London, 28 June - 2 July 2004 ECA Vol.**28G**, P-4.197 (2004)*

Inboard versus outboard pellet refuelling of MAST plasmas

K B Axon, G P Maddison, M N Price, R Scannell, S Shibaev, D Taylor,
D Terranova [1], M J Walsh [2]

EURATOM/UKAEA Fusion Association, Culham, Abingdon, Oxon. OX14 3DB, UK
[1] *Consorzio RFX - Associazione Euratom-Enea sulla Fusione, I-35127 Padova, Italy*
[2] *Walsh Scientific Ltd, Culham Science Centre, Abingdon, Oxon. OX14 3EB, UK*

1. Introduction - the MAST pellet injection system

Refuelling of tokamak plasmas over long time-scales remains a high-priority area of development not only for present experiments but especially for ITER. There are also advantages in being able to deliver new fuel particles directly inside either edge or internal transport barriers used to improve their performance. One system under investigation is therefore periodic injection of high-velocity pellets of frozen fuel isotopes. On MAST, deuterium pellet injection is being studied in spherical tokamak geometry using an eight-barrel (six currently in service) gas-propulsion launcher, supplied from Risø, Denmark / FOM, Netherlands. Individual temperature control of each barrel [1] allows three sizes of cylindrical pellets of equal diameter and length $1.1/1.35/1.7$ mm ($\approx 0.66/1.2/2.4\times10^{20}$ D atoms) to be fired, with variable delays ≥ 3 ms between each one. Two PTFE guide-tubes (4 mm internal diameter) deliver the pellets to either an outboard mid-plane port giving approximately radial entry into the plasma, or to a top port which directs them vertically through its inboard side (Fig.1). Respective lengths are 26.7 m and 18.0 m, minimum radii of curvature ≈ 2.5 m and ≈ 0.7 m (owing to clearance under the shield roof), with the more sinuous outboard line following a helical path to reduce pellet stresses. In addition two shorter test lines with comparable curvatures are incorporated. A switcher chooses one of these tracks between shots. Masses leaving the launcher and at the vessel end of the outboard guide-tube are measured using resonant microwave cavities, while velocities are measured with light sensors. Losses along bending flight-lines are characterized in Fig.2 , which shows

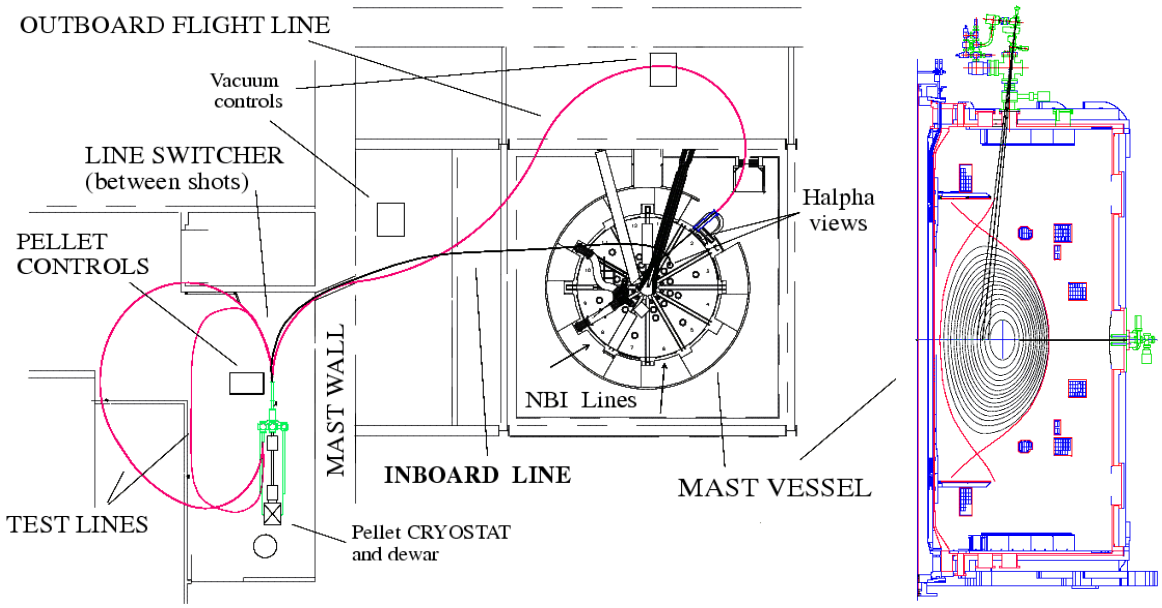

Fig.1 Top view (left) of inboard and outboard pellet tracks on MAST, plus side projection (right) of corresponding trajectories into a typical double-null plasma.

a linear fall with rising velocity in the fraction of initial pellet mass arriving into a known target volume at the end of one of the test lines. Also superimposed are ratios of the launcher microwave cavity signal alternatively to the one at the end of the outboard guide-tube, for both a test series, plus some of the pulses discussed below. Scatter / variability is evidently larger, while somewhat lower values are found, but at least for speeds $< 300\ \mathrm{m \cdot s^{-1}}$ there is no deterioration of transmission between multiple pellets fired into a single pulse (each different symbol). Pellet speeds $\approx 200 \rightarrow 300\ \mathrm{m \cdot s^{-1}}$ are typically adopted for both experimental flight-lines. Other pellet diagnostics include a high-speed video camera, plus two CCD "tracker" cameras provided by ENEA Padua, to image the ablation trajectories in the plasma.

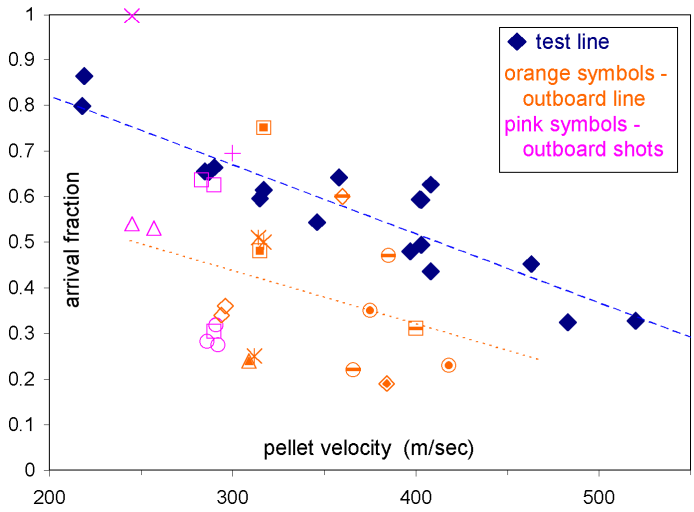

Fig.2 Fraction of pellet mass arriving at end of test line, as a function of velocity (blue diamonds). Also superimposed: equivalent data along outboard flight-line (orange), plus some of outboard pulses in text (pink) – each different symbol represents an individual shot.

2. Inboard versus outboard refuelling

Typical behaviour of pellet refuelled plasmas on MAST is illustrated in Fig.3 for a 0.76 MA, 0.53 T H-mode (#9234) with predominantly Ohmic ($\leq 30\%$ RF) heating into which a pair of inboard pellets are fired at $260\ \mathrm{m \cdot s^{-1}}$. Each pellet produces a substantial rise in line-average density, leading to a three-fold increase above the Greenwald level, $f_{\mathrm{Gwd}} \equiv \bar{n}_e / n_{\mathrm{Gwd}} \approx 1.16$. Here β_t from EFIT steadily declines throughout, indicating the rise is at best adiabatic. Changes in Dα ELM signatures also imply a return to L-mode. The lower contour plot from Thomson scattering at 200 Hz reveals that the pellets induce a very hollow density profile which persists for just over an energy confinement time (≈ 0.025 s). Penetration implied is approximately recovered in modelling with the NGS ablation code [2], which calculates that the majority of particles are deposited around normalized radius $(r/a) \approx 0.6$ for these parameters. Individual Thomson scattering profiles at the arrow in Fig.3 are compared with simultaneous safety factor profile from EFIT in Fig.4, which suggests the shoulders in the hollow density are closely aligned with the $q = {}^3/_2$ surface (note that absence of a $q = 1$ surface is consistent with the lack of sawteeth). A sudden, internal readjustment of the profile can be seen to occur at ≈ 0.218 s in Fig.3, leading to a much more centrally peaked density distribution. This prompt event has been observed in many of the pulses presented, but is as yet unexplained. For #9234, simultaneous magnetic activity remains quiescent, while soft X-ray emission only increases centrally in proportion to the core density.

In Ohmically-dominated plasmas, behaviour is similar also for matching outboard pellet injection. Large density increases up to $\approx 250\%$ are again observed, and sometimes maintained with little loss. Profiles are added in Fig.4 just after the first of two outboard pellets into an otherwise matching plasma which sustains $f_{\mathrm{Gwd}} \geq 1.16$ for the remainder of the pulse (#9419). As before, peaks in the initially prolonged hollow density profile appear well aligned with $q = {}^3/_2$, until a more centrally peaked distribution emerges through internal

rearrangement. In another example with lower central plasma temperature (≈ 650 eV initially), a similar outboard pellet at $300\,\mathrm{m\cdot s^{-1}}$ penetrated fully to its core, averting any hollow profile phase (#9206). Calculations with the NGS code [2] for these parameters do correspondingly find the axis is reached, with greatest deposition around $(r/a) \approx 0.35$.

Comparable plasmas at $0.76 \rightarrow 1.0$ MA with 1.25 MW of neutral beam additional heating tend to gain smaller increments in density $\leq 100\%$ and reach lower Greenwald fractions $f_{\mathrm{Gwd}} \approx 0.6 \rightarrow 0.8$ from up to four pellets, although β_t is better preserved. As noted for #9234 in Fig.3, pellets still tend to interrupt H-mode phases at this input power level (up to ≈ 2.8 MW total). Results are summarized in Fig.5 in terms of the instantaneous gross refuelling efficiency immediately following each pellet, estimated as $\varepsilon_g \approx \Delta N_e$/(pellet mass launched), and accompanying plasma refuelling efficiency $\varepsilon_p \approx \Delta N_e$/(pellet mass at vessel) for the outboard line, where $\Delta N_e = \Delta \bar{n}_e \times$ (plasma volume). This will overestimate plasma increments, but should preserve trends for fixed plasma shape. Although errors will be large, it is clear that ε_g tends to fall with input power for both inboard and outboard injection, but is systematically higher for the former, consistent with smaller losses along its shorter, straighter flight-line (see Fig.1). Closeness of both $\varepsilon_g^{\mathrm{in}}$ and $\varepsilon_p^{\mathrm{out}}$ to 100% for Ohmic cases in fact suggests inboard guide-tube losses are insignificant, and thus correspondence of $\varepsilon_g^{\mathrm{in}}$, $\varepsilon_p^{\mathrm{out}}$ generally implies there is no advantage in terms of plasma refuelling ε_p for either injection path over the range of conditions so far studied.

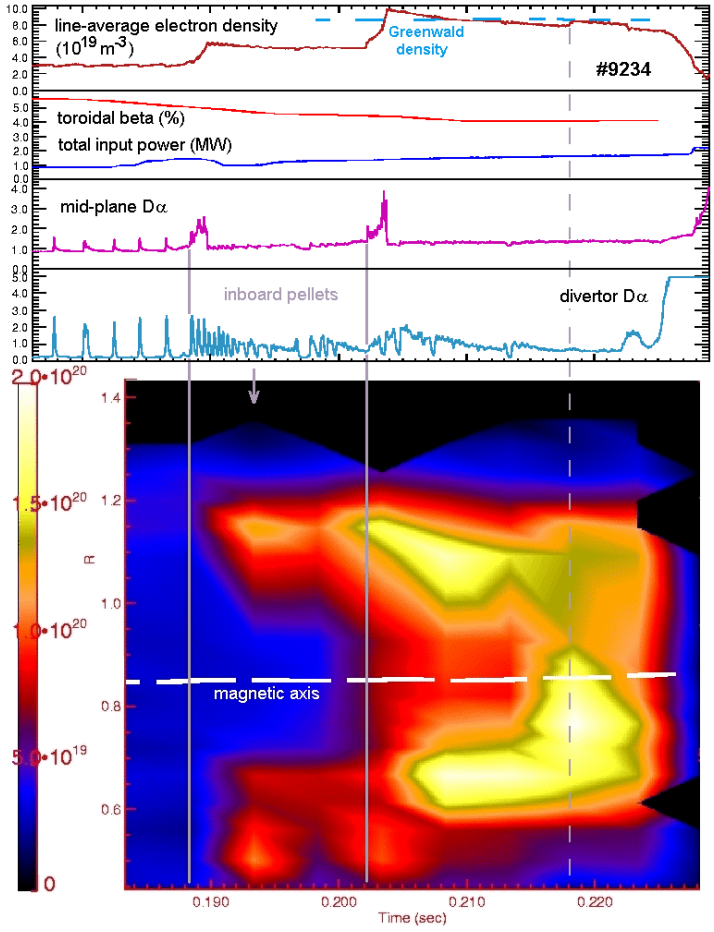

Fig.3 Interferometer, β_t, power, Dα signals, & density contour plot from Thomson scattering, for two inboard pellets injected into an Ohmically-dominated plasma.

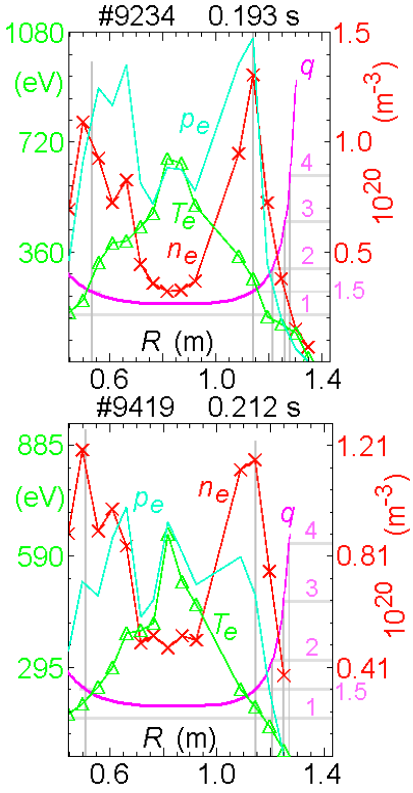

Fig.4 Comparison of Thomson scattering and EFIT q profiles for inboard pellets case in Fig.3 (top, at time shown by arrow), and matching example with outboard pellets (bottom).

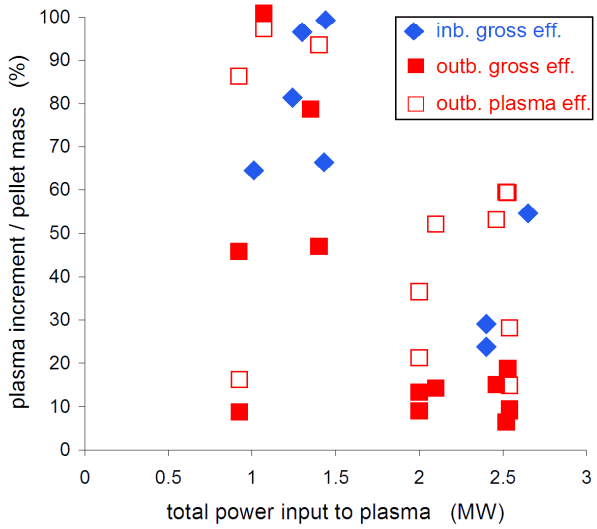

Fig.5 Refuelling efficiency immediately after each pellet against heating power: gross value for inboard / outboard entry; plasma value for outboard entry.

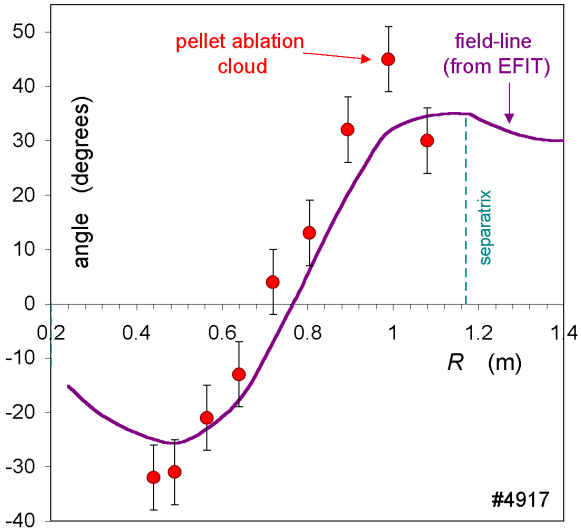

Fig.6 Measured orientation of ablation cloud for outboard injection compared with field-line angle from EFIT.

Fast visible imaging makes it possible to track orientation of the oblate pellet ablation cloud [3] as it traverses the plasma. In Fig.6 this measured inclination is compared with local field-line angle from EFIT, for outboard injection of a pellet at $395\,\mathrm{m\cdot s^{-1}}$ into a 0.55 MA Ohmic plasma. These conditions allow the pellet to travel across almost the whole plasma diameter, and from Fig.6 it is apparent that its local ablation emission remains closely aligned with field-line angle throughout. Pellet injection can hence simultaneously detect spatial profiles of field-line pitch, or $q(r)$, within the confined region.

3. Conclusions

Comparisons of inboard versus outboard pellet refuelling on MAST demonstrate that large increases in line-average plasma density, up to $\approx 250 \rightarrow 300\%$, can be produced, exceeding the Greenwald level for Ohmic conditions. For either line of entry, density gains and hence refuelling efficiency tend to decline with total heating power, though smaller flight-line losses yield a systematically higher gross value for inboard injection. Fuelling efficiencies in the plasma near 100% have been achieved in Ohmic cases using either path, while for a total input power with NBH of ≈ 2.8 MW best density increases of $\approx 100\%$, to Greenwald fractions of ≈ 0.8, have been obtained using inboard injection. At the present level of auxiliary power in MAST, pellets tend to cause a back-transition from H- to L- mode, accompanied by a fall or dip in normalized plasma pressure. This drop becomes smaller, however, for higher power. Hence pellet refuelling to higher density H-modes should become accessible in MAST at greater NB power (≤ 5 MW). Its recently-installed improved divertor has also been constructed with a steerable inboard guide-tube element, allowing trajectories to be varied over a high-field-side arc for further optimization of pellet effects.

This work was funded jointly by the UK Engineering & Physical Sciences Research Council and by EURATOM.

References

[1] S Shibaev & K B Axon Fusion Engineering & Design 66-68 (2003) 893
[2] L R Baylor *see* http://ornl.gov/sci/fed/pellet/NGSpellet.html
[3] R D Durst *et al* Review of Scientific Instruments 59 (1988) 1623